CrystEngComm

COMMUNICATION

Check for updates

Intrinsically porous molecular building blocks for metal organic frameworks tailored by the bridging effect of counter cations†

Peng Yang,[ab] Buthainah Alshankiti[a] and Niveen M. Khashab [iD] *[a]

Predesigned organic linkers have dominated the world of pillared metal organic frameworks to tune the overall morphology, size, and performance of this class of materials. However, the porosity of the framework was never guaranteed due to possible assembly interpenetration and ligand self-closure. Here, we present an interesting construction strategy employing macrocyclic molecular building blocks (MBBs) with intrinsic voids to boost the porosity and host-guest interactions of these hybrid frameworks. *In situ* co-crystallization of the isolated polyoxomolybdates ($P_2Mo_5O_{23}$) and cyclodextrins (CDs) has resulted in seven POM–CD MOFs following this strategy. The bridging effect dictated by the size of counter cations (Na^+, K^+, and Cs^+) can readily tune the structural and performance features of the end frameworks including pore morphology and water stability. This strategy paves the way for the precise design of customized porous materials with built-in macrocyclic hosts for improved molecular recognition of prospective guest molecules.

Inspired by the evolution of biological systems from simple units into a vast range of complex structures, scientists have directed their attention towards the rational design of self-organizing building blocks or supramolecular assembly of more intricate artificial systems. Developing superior smart materials has been pivotal to resolve industrial, environmental, and societal challenges.[1–4] The concept of preparing "materials on demand" or tailoring material design has fueled this field for the last decade.[5] Metal organic frameworks (MOFs) have proved to be a main player in this

field following the guidelines of reticular chemistry and the well-defined structures of their secondary building units (SBUs) or molecular building blocks (MBBs).[6] Aside from the many attractive features of MOFs (*e.g.*, huge surface area and low crystal density), construction of networks with tailored porosity and a prospective application have been the main highlight.[7–9]

A major drawback to the success of the rational and predesigned synthesis of robust porous materials has been the limited access to the pores within open structures.[10] This is a critical aspect to the utility of these structures and occurs due to either self-interpenetration[11] as observed for very open frameworks or strong host-guest interactions that lead to the destruction of the host framework when removal or exchange of guests is attempted.[12] As a result, the development of reliable and reproducible methods to achieve robust porous frameworks with tailored structures and tunable properties remains a considerable challenge.

The classical "pillar" construction principle, which mainly relies on synthesizing and tailoring the organic ligand, is the most used strategy for the precise modification of the pores and the topologies of MOFs (Fig. 1). Naturally occurring γ-cyclodextrin (γ-CD) have been successfully used in building CD-MOFs with permanent porosity and the ability to store small molecules in their pores.[13–15] Recently, we have communicated the use of CDs combined with inorganic polyoxometalates (POMs)[16–18] as MBBs to prepare a new generation of porous hybrid frameworks (POM–CD MOFs).[19] These assemblies benefited from the intrinsic microporosity and functional multiplicity of both isolated building blocks. This promoted a different strategy in the construction of porous frameworks by employing macrocyclic MBBs (Fig. 1). A library of customized porous structures could now be prepared on-demand by choosing the right macrocyclic MBBs. More importantly, we prove that mechanistically the counter cations do not only balance the charge, but play a critical role as "a bridge" to connect these building blocks. We investigated the bridging effect of different counter cations of

[a] Smart Hybrid Materials Research Group (SHMs), Advanced Membranes and Porous Materials Center (AMPMC), King Abdullah University of Science and Technology (KAUST), Thuwal 23955, Saudi Arabia.
E-mail: niveen.khashab@kaust.edu.sa
[b] College of Chemistry and Chemical Engineering, Hunan University, Changsha 410082, P.R. China

† Electronic supplementary information (ESI) available. CCDC 1963899, 1963900 and 1963902–1963906. For ESI and crystallographic data in CIF or other electronic format see DOI:10.1039/d0ce00397b
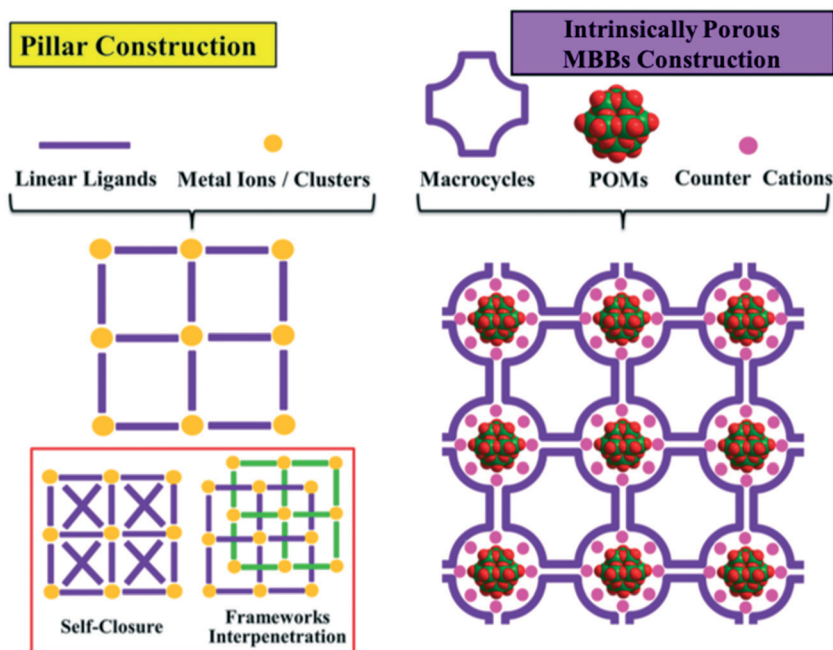
Fig. 1 Illustration of the pillar and intrinsically porous MBBs construction strategies in MOF chemistry.

alkali metals (Na^+, K^+, and Cs^+), of which the size had a direct effect on the structural features of the corresponding POM–CD MOFs, for example, porosity factors and pore shape.

Results and discussion

All seven compounds were synthesized by the reaction of CDs with 85% H_3PO_4 and $Na_2MoO_4 \cdot 2H_2O$ in acetate buffers involving different alkali metal ions (e.g., Na^+, K^+, and Cs^+), and isolated as protonated single/mixed cation salts $H_2Na_{22}[P_2Mo_5O_{23}]_4[\alpha\text{-CD}]_4 \cdot 7CH_3COOH \cdot 48H_2O$ (**Na-PMo-α-CD**), $H_{2.5}K_{11.5}Na_{10}[P_2Mo_5O_{23}]_4[\alpha\text{-CD}]_4 \cdot CH_3COOH \cdot 35H_2O$ (**K-PMo-α-CD**), $H_{1.5}Cs_{4.5}Na_6[P_2Mo_5O_{23}]_2[\alpha\text{-CD}]_2 \cdot 3CH_3COOH \cdot 30H_2O$ (**Cs-PMo-α-CD**), $H_5Na_{19}[P_2Mo_5O_{23}]_4[\beta\text{-CD}]_4 \cdot 2CH_3COONa \cdot 42H_2O$

(**Na-PMo-β-CD**), $H_3Na_{21}[P_2Mo_5O_{23}]_4[\gamma\text{-CD}]_2 \cdot 7CH_3COONa \cdot 56H_2O$ (**Na-PMo-γ-CD**), $H_4K_{20}Na_2[P_2Mo_5O_{23}]_4[\gamma\text{-CD}]_2 \cdot 2(CH_3COO) \cdot 48H_2O$ (**K-PMo-γ-CD**), and $H_{3.5}Cs_{5.5}Na_6[P_2Mo_5O_{23}]_2[\gamma\text{-CD}] \cdot 3(CH_3COO) \cdot 37H_2O$ (**Cs-PMo-γ-CD**), respectively.

Self-assembly of the in situ formed $\{P_2Mo_5O_{23}\}$ (P_2Mo_5) with α-CD in $NaCH_3COO/CH_3COOH$ buffer (pH 4) has resulted in a three-dimensional (3D) framework of **Na-PMo-α-CD** as seen by X-ray structural analysis (Fig. 2). The asymmetric unit is composed of four crystallographically independent α-CDs and P_2Mo_5 ligated mainly by Na^+ cations, of which the coordination spheres are fulfilled by oxygen atoms from the hydroxy groups of α-CDs and terminal oxygens of P_2Mo_5 in concert with water molecules. As viewed from a axis, the skeleton of **Na-PMo-α-CD** is built upon

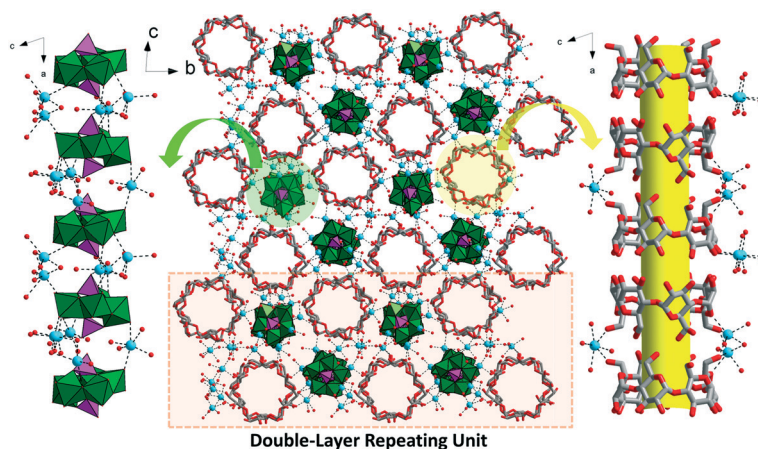**Fig. 2** Combined polyhedral/ball-and-stick representation of **Na-PMo-α-CD**. Color code: MoO_6, green octahedra; PO_4 pink tetrahedra; Na, turquoise; O, red; C, gray.

separate chain-like structures that are constructed by P_2Mo_5 and α-CD moieties, respectively, stabilized by Na···O and hydrogen bonds (Fig. 2 and S1a†). Such chains pack by themselves alternatively to weave a layer of ABAB mode along b axis. The staggered overlap of adjacent layers outputs a double layer with a certain offset distance, which behaves as the basic repeating entity and piles up along the c axis to give rise to a 3D scaffold *via* sharing the cations in between. With deeper insight into the CD chains, all CDs adopt head to head/end to end connection modes to yield hollow tubes (Fig. S1b†), where a few acetate functions are accommodated in to complete the host–guest assembly (Fig. S2†), resulting in the porous character of the whole framework.

Introduction of the larger K^+ or Cs^+ cations into the scenario of **Na-PMo-α-CD** gave rise to similar frameworks, namely, **K-PMo-α-CD** and **Cs-PMo-α-CD**. Interestingly, close examination of the P_2Mo_5 species in one double-layer repeating unit unveils that, possibly because of the increasing size of the counter cations scattered among the confined space area, the two neighbouring P_2Mo_5 have been pushed closer with the distance decreasing from 12.52 Å (**Na-PMo-α-CD**) *via* 10.02 Å (**K-PMo-α-CD**) to 9.78 Å (**K-PMo-α-CD**), saving room for extra CDs per their unit cells (Fig. 3). Also, supported by the data given by PLATON, "the total potential solvent accessible void volume divided by their respective unit cell volume" was increased from 14.1% (1174.6/8311.3 Å^3, **Na-PMo-α-CD**) *via* 15.4% (2490.1/16191.1 Å^3, **K-PMo-α-CD**) to 18.1% (2867.5/15855.1 Å^3, **Cs-PMo-α-CD**), indicating that the bridging effect of the counter cations could effectively tune the porosity of POM–CD MOFs.

Intrigued by the bridging effect of the counter cations, we set about exploring the structural influence provided by homologous CDs. Single-crystal XRD reveals that, albeit the same Na^+ cation media, the size of CD macrocycles could heavily impact the detailed structural arrangement of the inorganic/organic MBBs in **Na-PMo-β-CD** and **Na-PMo-γ-CD** as

well. Except for the shrinking distance between the two nearest P_2Mo_5 from 12.52 Å (**Na-PMo-α-CD**) to 9.21 Å (**Na-PMo-γ-CD**), in particular, the interlaced P_2Mo_5 couples could be re-arranged to transfer from double units (**Na-PMo-α-CD** and **Na-PMo-β-CD**) to single layers (**Na-PMo-γ-CD**) by the help of the squeezing stemming from the increased diameter of CDs (Fig. 4). Moreover, as calculated by PLATON, the total potential solvent accessible void volume gradually increases from 1174.6 Å^3 (**Na-PMo-α-CD**) *via* 1923.7 Å^3 (**Na-PMo-β-CD**) to 4262.9 Å^3 (**Na-PMo-γ-CD**).

Of further interest, the interplay of the two impacts, the bridging effect of cations and the "fitting" of CDs in the framework, has been investigated in succession. By means of introducing K^+ or Cs^+ cations into the **Na-PMo-γ-CD** system, two similar frameworks have been identified in **K-PMo-γ-CD** and **Cs-PMo-γ-CD**. However, by sharp contrast to the group of **Na/K/Cs-PMo-α-CD**, herein, the larger size of cations could not push the nearby P_2Mo_5 closer, as indicated by their almost identical distances (9.21 Å (**Na-PMo-γ-CD**), 9.30 Å (**K-PMo-γ-CD**), and 9.41 Å (**Cs-PMo-γ-CD**)). Also, as verified by PLATON, the three frameworks bear similar percent of void (16.5%, **Na-PMo-γ-CD**; 16.9%, **K-PMo-γ-CD**; and 17.2%, **Cs-PMo-γ-CD**). Instead, the K^+ or Cs^+ ions are capable of flattening some of the flexible γ-CD toroids, and the obvious pore-shape distortion could be demonstrated by the aspect ratio of the original γ-CD (1.006) and the ones undergoing more bridging (0.790) or in other words squeezed to fit in the framework (Fig. 5). Therefore, it could be summarized that the nature of the CDs can influence the overall structural patterns, while counter cations could precisely tune the regional features of the frameworks, such as pore size and shape.

Apart from the aforementioned structural tunability, it is worth to stress the distinct characters of each CD analogue in the synthetic strategies of the PMo–CD MOFs. The family of **Na/K/Cs-PMo-α-CD**, for example, could be obtained at pH 4 rather than pH 5. It is presumed that the pH < pK_a (HOAc,
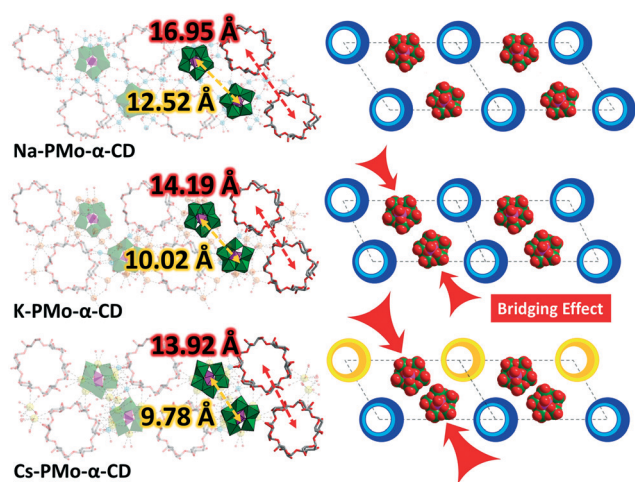

Fig. 3 The distance between the two nearest P_2Mo_5 units affected by the bridging effect of counter cations. The α-CD toroids bearing opposite directions are highlighted in yellow and blue color, respectively.
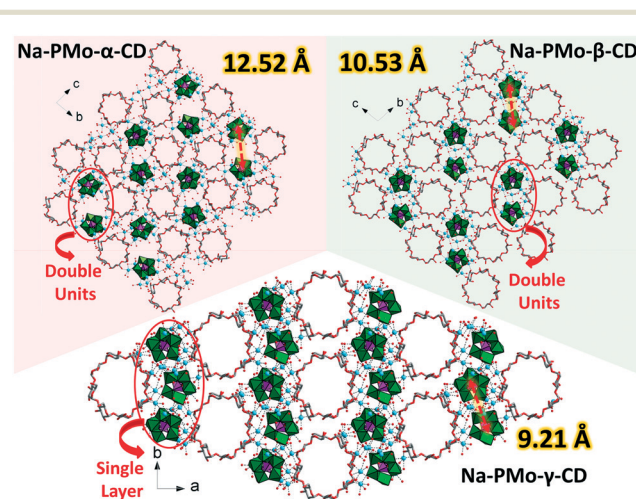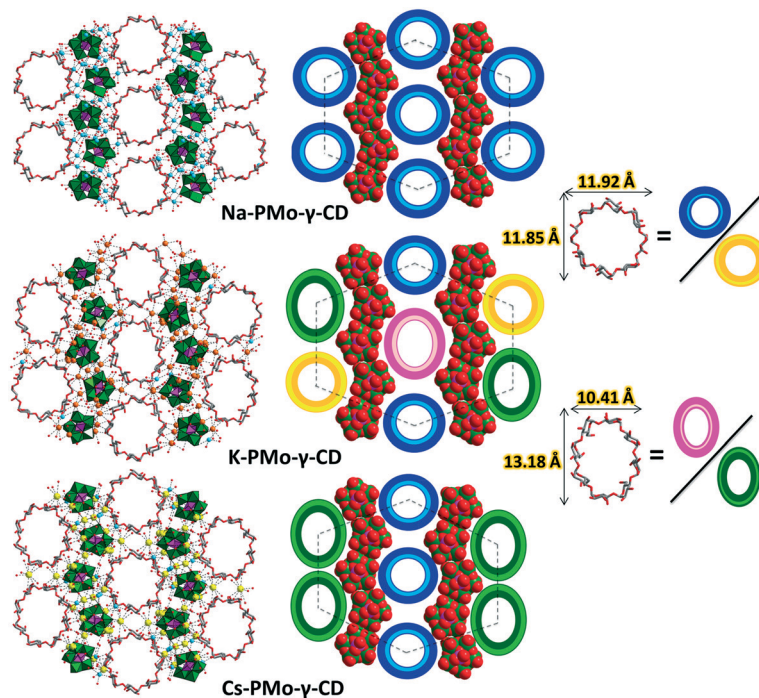

Fig. 4 Structural re-arrangement of MBBs in Na-PMo-CD MOFs affected by the size of CD analogues.

Fig. 5 Pore-shape distortion affected by the bridging effect of counter cations in **Na/K/Cs-PMo-γ-CD**. Different aspect ratios and orientations of γ-CDs have been highlighted by various colors (distorted pink and green).

pK_a 4.76) could strengthen the multiple hydrogen bonding interactions between the accommodated HOAc guest molecules and the hydroxy groups of α-CD hosts, thereby stabilizing the whole frameworks. Being verified by FT-IR spectra (Fig. S3–S5†), the adsorption peak centered at 1710 cm^{-1} declares the presence of HOAc molecules rather than acetate salts in the solid states of **Na/K/Cs-PMo-α-CD**. As to **Na-PMo-β-CD**, it could be prepared under both pH 4 and 5, but in Na$^+$-containing media only. The appearance of K$^+$ or Cs$^+$ would precipitate the β-CD rapidly which could be assigned to its low water solubility (18.5 g L^{-1}, 25 °C). Finally for **Na/K/Cs-PMo-γ-CD**, the same structures could be obtained under single/mixed cation environments at both pH 4 and 5, which might be ascribed to the uniform layered pattern of P$_2$Mo$_5$, featuring better environmental compatibility in the crystal lattices than the embedded coupled dimer of **Na/K/Cs-PMo-α-CD** and **Na-PMo-β-CD**. Moreover, in spite of the good stability of these PMo-CD MOFs in most common organic solvents (*e.g.*, methanol, acetone, and acetonitrile), the Na/K-PMo-CD MOFs could easily decompose in water as confirmed by NMR studies (Fig. S6–S11†). However, the large cations of Cs$^+$ could remarkably enhance the stability of the framework of **Cs-PMo-γ-CD** in aqueous media (Fig. S12†), which could be explained by the "normal solubility trend" in POM chemistry.[20]

Conclusions

Without the tedious synthesis of new organic ligands required for the classical pillared MOF synthesis, the intrinsically porous MBBs construction strategy paves the way for a facile approach not only for the rational design of molecular-level controlled porous materials, but also for their property optimization and function expansion. Our research results show that the size of counter cations could easily program the structural features of POM–CD MOFs as well as their water stability. Using Cs$^+$ cations, the framework showed an enhanced water stability in addition to selective guest molecules separation by the distortional CD macrocycles. This strategy can be furthermore expanded to include other macrocycles such as cucurbiturils and pillararenes, of which the frameworks have been already acquired and will be the subject of future reports.

Methods

Experimental results (crystallographic data, elemental analysis, FT-IR spectra, TGA diagrams, powder XRD patterns, multinuclear (^{1}H, ^{13}C, and ^{31}P) NMR spectra) can be found in the Supplementary Information.

Synthesis of H$_2$Na$_{22}$[P$_2$Mo$_5$O$_{23}$]$_4$[α-CD]$_4$·7CH$_3$COOH·48H$_2$O (Na-PMo-α-CD)

To a solution of α-cyclodextrin (0.097 g, 0.100 mmol) in 5 mL 1 M NaCH$_3$COO/CH$_3$COOH buffer (pH 4.0), 85% H$_3$PO$_4$ (50 μL), and Na$_2$MoO$_4$·2H$_2$O (0.242 g, 1.000 mmol) were added successively upon stirring. The solution was then stirred for 1 hour at 80 °C. The clear colorless solution was cooled to room temperature, filtered, and the filtrate was allowed to evaporate in an open vial at room temperature. The block-

shaped colorless crystalline product **Na-PMo-α-CD** started to appear after four weeks and was collected by filtration and then air-dried. Yield: 0.172 g (74% based on α-CD).

Synthesis of H$_{2.5}$K$_{11.5}$Na$_{10}$[P$_2$Mo$_5$O$_{23}$]$_4$[α-CD]$_4$·CH$_3$COOH ·35H$_2$O (K-PMo-α-CD)

The compound was prepared by exactly the same procedure of **Na-PMo-α-CD**, but with 1 M KCH$_3$COO/CH$_3$COOH buffer (pH 4.0) instead of 1 M NaCH$_3$COO/CH$_3$COOH buffer (pH 4.0). The block-shaped colorless crystalline product **K-PMo-α-CD** started to appear after four weeks and was collected by filtration and then air-dried. Yield: 0.160 g (72% based on α-CD).

Synthesis of H$_{1.5}$Cs$_{4.5}$Na$_6$[P$_2$Mo$_5$O$_{23}$]$_2$[α-CD]$_2$·3CH$_3$COOH ·30H$_2$O (Cs-PMo-α-CD)

To a solution of α-cyclodextrin (0.097 g, 0.100 mmol) in 5 mL 1 M NaCH$_3$COO/CH$_3$COOH buffer (pH 4.0), 85% H$_3$PO$_4$ (100 μL), Na$_2$MoO$_4$·2H$_2$O (0.242 g, 1.000 mmol), and CsCl (0.168 g, 1.000 mmol) were added successively upon stirring. The solution was then stirred for 1 hour at 80 °C. The turbid white solution was cooled to room temperature, filtered, and the filtrate was allowed to evaporate in an open vial at room temperature. The block-shaped colorless crystalline product **Cs-PMo-α-CD** started to appear after three weeks and was collected by filtration and then air-dried. Yield: 0.159 g (61% based on α-CD).

Synthesis of H$_5$Na$_{19}$[P$_2$Mo$_5$O$_{23}$]$_4$[β-CD]$_4$·2CH$_3$COONa·42H$_2$O (Na-PMo-β-CD)

To a solution of β-cyclodextrin (0.113 g, 0.100 mmol) in 5 mL 1 M NaCH$_3$COO/CH$_3$COOH buffer (pH 5.0), 85% H$_3$PO$_4$ (50 μL), and Na$_2$MoO$_4$·2H$_2$O (0.242 g, 1.000 mmol) were added successively upon stirring. The solution was then stirred for 1 hour at 80 °C. The clear colorless solution was cooled to room temperature, filtered, and the filtrate was allowed to evaporate in an open vial at room temperature. The block-shaped colorless crystalline product **Na-PMo-β-CD** started to appear after five weeks and was collected by filtration and then air-dried. Yield: 0.160 g (67% based on β-CD).

Synthesis of H$_3$Na$_{21}$[P$_2$Mo$_5$O$_{23}$]$_4$[γ-CD]$_2$·7CH$_3$COONa·56H$_2$O (Na-PMo-γ-CD)

To a solution of γ-cyclodextrin (0.130 g, 0.100 mmol) in 5 mL 1 M NaCH$_3$COO/CH$_3$COOH buffer (pH 5.0), 85% H$_3$PO$_4$ (50 μL), and Na$_2$MoO$_4$·2H$_2$O (0.242 g, 1.000 mmol) were added successively upon stirring. The solution was then stirred for 1 hour at 80 °C. The clear colorless solution was cooled to room temperature, filtered, and the filtrate was allowed to evaporate in an open vial at room temperature. The needle-shaped colorless crystalline product **Na-PMo-γ-CD** started to appear after three weeks and was collected by filtration and then air-dried. Yield: 0.282 g (68% based on γ-CD).

Synthesis of H$_4$K$_{20}$Na$_2$[P$_2$Mo$_5$O$_{23}$]$_4$[γ-CD]$_2$·2(CH$_3$COO)·48H$_2$O (K-PMo-γ-CD)

The compound was prepared by exactly the same procedure of **Na-PMo-γ-CD**, but with 1 M KCH$_3$COO/CH$_3$COOH buffer (pH 5.0) instead of 1 M NaCH$_3$COO/CH$_3$COOH buffer (pH 5.0). The needle-shaped colorless crystalline product **K-PMo-γ-CD** started to appear after two weeks and was collected by filtration and then air-dried. Yield: 0.281 g (70% based on γ-CD).

Synthesis of H$_{3.5}$Cs$_{5.5}$Na$_6$[P$_2$Mo$_5$O$_{23}$]$_2$[γ-CD]·3(CH$_3$COO) ·37H$_2$O (Cs-PMo-γ-CD)

To a solution of γ-cyclodextrin (0.130 g, 0.100 mmol) in 5 mL 1 M NaCH$_3$COO/CH$_3$COOH buffer (pH 5.0), 85% H$_3$PO$_4$ (100 μL), Na$_2$MoO$_4$·2H$_2$O (0.242 g, 1.000 mmol), and CsCl (0.051 g, 0.300 mmol) were added successively upon stirring. The solution was then stirred for 1 hour at 80 °C. The turbid white solution was cooled to room temperature, filtered, and the filtrate was allowed to evaporate in an open vial at room temperature. The needle-shaped colorless crystalline product **Cs-PMo-γ-CD** started to appear after two weeks and was collected by filtration and then air-dried. Yield: 0.280 g (58% based on γ-CD).

Author contributions

N. M. K. conceived the idea. P. Y. and B. A. carried out the synthesis and characterization experiments. P. Y. and N. M. K. designed the experiments and wrote the paper.

Conflicts of interest

The authors declare no competing interest.

References

1 I. Cobo, M. Li, B. S. Sumerlin and S. Perrier, Smart hybrid materials by conjugation of responsive polymers to biomacromolecules, *Nat. Mater.*, 2015, **14**, 143–159.

2 M. A. English, *et al.*, Programmable CRISPR-responsive smart materials, *Science*, 2019, **365**, 780–785.

3 R. Kumar, *et al.*, Revisiting fluorescent calixarenes: from molecular sensors to smart materials, *Chem. Rev.*, 2019, **119**, 9657–9721.

4 X. Yan, *et al.*, A multiresponsive, shape-persistent, and elastic supramolecular polymer network gel constructed by orthogonal self-assembly, *Adv. Mater.*, 2012, **24**, 362–369.

5 M. J. Kalmutzki, N. Hanikel and O. M. Yaghi, Secondary building units as the turning point in the development of the reticular chemistry of MOFs, *Sci. Adv.*, 2018, **4**, eaat9180.

6 O. M. Yaghi, *et al.*, Reticular synthesis and the design of new materials, *Nature*, 2003, **423**, 705–714.

7 S. C. Mckellar, *et al.*, Pore shape modification of a microporous metal−organic framework using high pressure: accessing a new phase with oversized guest molecules, *Chem. Mater.*, 2016, **28**, 466–473.

8 Z. R. Herm, *et al.*, Separation of hexane isomers in a metal-organic framework with triangular channels, *Science*, 2013, **340**, 960–964.

9 J.-M. Lin, *et al.*, A metal–organic framework with a pore size/shape suitable for strong binding and close packing of methane, *Angew. Chem., Int. Ed.*, 2016, **55**, 4674–4678.

10 M. Eddaoudi, *et al.*, Modular chemistry: secondary building units as a basis for the design of highly porous and robust metal-organic carboxylate frameworks, *Acc. Chem. Res.*, 2001, **34**, 319–330.

11 S. R. Batten and R. Robson, Interpenetrating nets: ordered, periodic entanglement, *Angew. Chem., Int. Ed.*, 1998, **37**, 1460–1494.

12 O. M. Yaghi, H. Li, C. Davis, D. Richardson and T. L. Groy, Synthetic strategies, structure patterns, and emerging properties in the chemistry of modular porous solids, *Acc. Chem. Res.*, 1998, **31**, 474–484.

13 R. A. Smaldone, *et al.*, Metal−Organic Frameworks from Edible Natural Products, *Angew. Chem., Int. Ed.*, 2010, **49**, 8630–8634.

14 R. S. Forgan, *et al.*, Nanoporous Carbohydrate Metal−Organic Frameworks, *J. Am. Chem. Soc.*, 2012, **134**, 406–417.

15 H. A. Patel, *et al.*, Noninvasive Substitution of K+ Sites in Cyclodextrin Metal-Organic Frameworks by Li+ Ions, *J. Am. Chem. Soc.*, 2017, **139**, 11020–11023.

16 D. L. Long, R. Tsunashima and L. Cronin, Polyoxometalates: Building Blocks for Functional Nanoscale Systems, *Angew. Chem., Int. Ed.*, 2010, **49**, 1736–1758.

17 H. N. Miras, J. Yan, D. L. Long and L. Cronin, Engineering Polyoxometalates with Emergent Properties, *Chem. Soc. Rev.*, 2012, **41**, 7403–7430.

18 U. Kortz, *et al.*, Polyoxometalates: Fascinating Structures, Unique Magnetic Properties, *Coord. Chem. Rev.*, 2009, **253**, 2315–2327.

19 P. Yang, *et al.*, Polyoxometalate−cyclodextrin metal−organic frameworks: from tunable structure to customized storage functionality, *J. Am. Chem. Soc.*, 2019, **141**, 1847–1851.

20 A. Misra, K. Kozma, C. Streb and M. Nyman, Beyond charge balance: counter-cations in polyoxometalate chemistry, *Angew. Chem., Int. Ed.*, 2019, **58**, 2–19.